

The peculiarities of the specific heat and dielectric permittivity related to the grain size distribution in ferroelectric nanomaterials

This article has been downloaded from IOPscience. Please scroll down to see the full text article.

2004 J. Phys.: Condens. Matter 16 6779

(<http://iopscience.iop.org/0953-8984/16/37/014>)

View [the table of contents for this issue](#), or go to the [journal homepage](#) for more

Download details:

IP Address: 129.252.86.83

The article was downloaded on 27/05/2010 at 17:33

Please note that [terms and conditions apply](#).

# The peculiarities of the specific heat and dielectric permittivity related to the grain size distribution in ferroelectric nanomaterials

M D Glinchuk<sup>1</sup> and P I Bykov<sup>2</sup>

<sup>1</sup> Institute for Problems of Materials Science, NASc of Ukraine, Kijijanovskogo 3, 03680 Kiev 142, Ukraine

<sup>2</sup> Radiophysics Faculty of Taras Shevchenko National University of Kiev, 2, Academician Glushkov Avenue Building # 5, 03127 Kiev, Ukraine

E-mail: dep4@materials.kiev.ua (M D Glinchuk)

Received 1 June 2004, in final form 11 August 2004

Published 3 September 2004

Online at [stacks.iop.org/JPhysCM/16/6779](http://stacks.iop.org/JPhysCM/16/6779)

doi:10.1088/0953-8984/16/37/014

## Abstract

We have performed calculations of the size effect in the temperature dependence of the BaTiO<sub>3</sub> nanograin ceramic specific heat and dielectric permittivity. We took into account the distribution of grain sizes that exists in any real nanomaterial. This distribution led to a distribution of the temperatures of the size driven transition from the ferroelectric to the paraelectric phase because of the relation between the temperature and the size. We calculated the transition temperature distribution function on the basis of the size distribution function. This function allows us to calculate the temperature dependence of any physical quantity for a nanomaterial. As examples, we calculated the specific heat and dielectric permittivity for nanograin ferroelectric ceramics. The results demonstrate the strong influence of the size distribution on the observed properties and especially on the values of the critical size and temperature extracted from experiment. We carried out a comparison of the theory with the measured specific heat and dielectric permittivity for BaTiO<sub>3</sub> nanomaterial. The theory developed described the experimental data fairly well. The possibility of extracting size distribution function parameters as well as real values of critical parameters from experimental data is discussed.

## 1. Introduction

The anomalies in the physical properties of nanomaterials, namely nanoparticle powders and nanograin ceramics, are attracting growing interest from scientists and engineers because of the size effects of properties useful for applications [1–3]. For ferroelectric nanomaterials the most important size effect is known to be the transformation of the ferroelectric phase

into a paraelectric one at some critical size [4]. Investigations of this phenomenon have been performed experimentally and theoretically in several works (see e.g. [5–7]). However, most of these works were devoted to the investigation of dielectric properties. The first experimental studies of the thermal properties (e.g. the specific heat) of BaTiO<sub>3</sub> polycrystalline thin film and nanograin thick film were published only recently [8–10]. Two main effects were revealed, namely the temperature of the specific heat jump appeared to be dependent on the average film thickness or nanoparticle size and there was a distribution of these temperatures: the width became larger with temperature decrease. The position of the maximum of this distribution was reasonably supposed to be related to the temperature of the size driven ferroelectric–paraelectric phase transition. The empirical expression for the dependence of the transition temperature on the average particle size was derived from experimental points. The physical mechanisms which led to this expression and to the distribution of the transition temperatures were not discussed in [8–10]. Measurements of the dependence of the dielectric permittivity on the average grain size in BaTiO<sub>3</sub> nanograin ceramics reveal the ‘puzzle’ of a much larger (about ten times larger) value of the critical size in the ceramics than in the nanopowder [11]. Up to now the physical reasons for this large difference have been unclear.

In the present paper we describe the main experimental results concerning size effects of the specific heat and dielectric susceptibility in nanograin BaTiO<sub>3</sub> on the basis of the equations obtained by us earlier [5]. We took into account also the distribution of the particle sizes, which exists in all nanomaterials. We showed that this distribution leads to a distribution of the transition temperatures. It was shown that all observed properties must be smeared and their maxima positions shifted by these distributions. The theory developed describes the specific heat temperature dependence and the dielectric permittivity size dependence observed for nanograin BaTiO<sub>3</sub> ceramics fairly well.

## 2. The theoretical description of the specific heat in nanomaterials

The calculation of nanomaterial properties has in the past been performed in the phenomenological theory framework on the basis of free energy functional variation (see e.g. [6]). This procedure leads to a differential Euler–Lagrange equation with boundary conditions originating from the surface energy. In the majority of the papers on this, the solution of the equation and the calculations of some dielectric properties are performed numerically. A method of analytical calculation was proposed recently [5] (see also [12, 13]). It was shown that the properties can be obtained by minimization of the conventional type of free energy, but with a coefficient of the squared polarization depending on the particle size, the temperature, the contribution of the depolarization field and the extrapolation length.

This free energy view is expressed as follows [5]:

$$F = \frac{A_R}{2} P^2 + \frac{B_R}{4} P^4 + \frac{C_R}{6} P^6 - P \cdot E. \quad (1)$$

Here  $P$  is averaged over the nanoparticle volume polarization,  $E$  is the external electric field,  $B_R \approx b$ ,  $C_R \approx c$ , where  $b$  and  $c$  are the corresponding constants of the bulk material. The renormalized coefficient  $A_R$  has the form

$$A_R \approx \alpha \cdot (T - T_{cl}(R)), \quad (2)$$

where  $\alpha$  is the inverse Curie–Weiss constant of the bulk,  $R$  is the size of the spherical nanoparticles.

The temperature of the size driven phase transition  $T_{cl}$  can be approximately written as

$$T_{cl}(R) \approx T_c \left( 1 - \frac{R_{cr}(0)}{R} \right), \quad (3)$$

$$R_{\text{cr}}(T) \approx \frac{R_{\text{cr}}(0)}{1 - \frac{T}{T_c}}. \quad (4)$$

Here  $T_{\text{cl}}(R)$  and  $R_{\text{cr}}(T)$  are the critical temperature and radius of the phase transition at some arbitrary radius  $R$  and temperature  $T$  respectively,  $T_c$  is the phase transition temperature of the bulk material. Substitution of equations (3), (4) into equation (2) transforms  $A_R$  into

$$A_R \approx \alpha(T - T_c) \left(1 - \frac{R_{\text{cr}}(T)}{R}\right). \quad (5)$$

Equations (2)–(5) allow us to calculate the temperature and size dependence for all nanomaterial properties averaged over the particle volume by conventional minimization of the free energy (1).

For example, the dielectric permittivity has the form

$$\varepsilon_{\text{PE}}(T, R) = \begin{cases} \frac{\varepsilon_0}{(R_{\text{cr}}(T)/R - 1)}, & R < R_{\text{cr}}, \\ \frac{1}{\alpha(T - T_{\text{cl}})}, & T > T_{\text{cl}}, \end{cases} \quad (6a)$$

$$\varepsilon_{\text{FE}}(T, R) = \begin{cases} \frac{\varepsilon_0}{2(1 - R_{\text{cr}}(T)/R)}, & R > R_{\text{cr}}, \\ \frac{1}{2\alpha(T_{\text{cl}} - T)}, & T < T_{\text{cl}}, \end{cases} \quad (6b)$$

$$\varepsilon_0 = \frac{1}{\alpha(T_c - T)},$$

where  $\varepsilon_{\text{PE}}$  and  $\varepsilon_{\text{FE}}$  are respectively the permittivities in the paraelectric and ferroelectric phases, and the first and second lines following the braces can be used respectively at some fixed temperature and radius. Keeping in mind that we are interested in consideration of the thermal capacity  $C_p$  of BaTiO<sub>3</sub>, let us write  $C_p$  for the first-order phase transition on the basis of equations (1), (2). Taking  $C_p = -T \frac{d^2\Phi}{dT^2}$ , one obtains the difference  $C_p(T < T_{\text{cl}}) - C_p(T > T_{\text{cl}}) \equiv \Delta C_p$  in the form

$$\Delta C_p = \frac{\alpha^2}{2b} \frac{T}{\sqrt{1 + \frac{4\alpha c}{b^2}(T_{\text{cl}}(R) - T)}}, \quad T < T_{\text{cl}}. \quad (7)$$

Note that for the first-order phase transition, the transition temperature  $T_{\text{cl}}$  used in the second-order phase transition in the form of equation (3) has to be shifted by  $\Delta T = \frac{3}{16} \frac{b^2}{\alpha c}$  [5].

### 3. The distribution function of the transition temperature

In real nanomaterials the sizes of nanoparticles are usually distributed, the form and parameters of the distribution function being dependent on the sample preparation technique. Let us suppose that the distribution function of radius  $R$  has a Gaussian form, namely

$$f(R) = C \exp\left(-\left(\frac{R - R_0}{\sigma}\right)^2\right), \quad 0 \leq R \leq \infty, \quad (8a)$$

where  $C$  is a normalization constant:

$$C = \frac{2}{\sigma \sqrt{\pi} (\text{erf}\left(\frac{R_0}{\sigma}\right) + 1)}. \quad (8b)$$

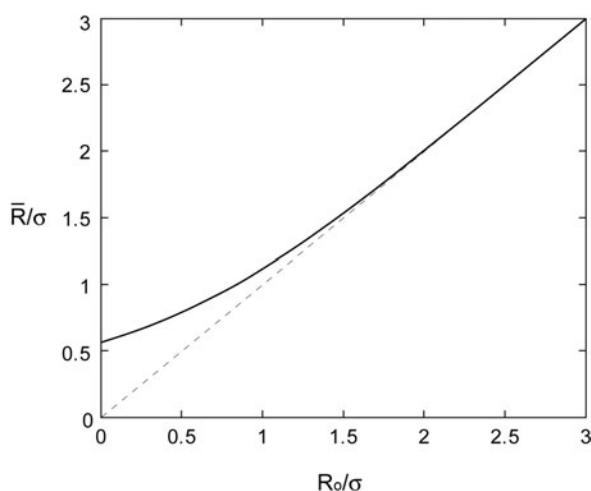


**Figure 1.** The dependence of the average grain size  $\bar{R}$  on the most probable grain size  $R_0$  and the dispersion parameter  $\sigma$ .

In equations (8),  $R_0$  and  $\sqrt{\ln 2}\sigma$  are respectively the most probable radius and the half-width at half-height. Because in many experimental works the average radius  $\bar{R}$  of the nanoparticles (obtained e.g. on the basis of an x-ray diffraction method) is given, it is useful to write out the relation between  $\bar{R}$  and  $R_0$ :

$$\bar{R} = R_0 + \frac{\sigma \exp\left(-\frac{R_0}{\sigma}\right)^2}{\sqrt{\pi} \left(1 + \operatorname{erf}\left(\frac{R_0}{\sigma}\right)\right)}. \quad (9)$$

In figure 1 one can see that  $\bar{R} \approx R_0$  at  $\frac{R_0}{\sigma} \geq 1.5$ , while at smaller values there is a difference between them. In particular, at  $R_0 \rightarrow 0$  the value  $\frac{\bar{R}-R_0}{\sigma} \rightarrow \frac{1}{\sqrt{\pi}}$ .

It follows from equation (3) that the distribution of the radius must be the source of the distribution of the transition temperatures  $T_{cl}$ . In accordance with the theory of probability [14], the distribution function  $F(T_{cl})$  can be expressed via  $f(R)$  in the following way:

$$F(T_{cl}) = f(R) \left| \frac{dR}{dT_{cl}} \right|. \quad (10)$$

Equation (10), incorporating equations (3), (8), yields

$$F(T_{cl}) = C_1 \frac{R_{cr}(0)T_c}{(T_c - T_{cl})^2} \exp\left(-\frac{R_{cr}^2(0)T_c^2}{\sigma^2} \left(\frac{1}{T_c - T_{cl}} - \frac{1}{T_c - T_{cl}^0}\right)^2\right), \quad (11a)$$

$$C_1 = \frac{2}{\sigma \sqrt{\pi} \left(1 + \operatorname{erf}\left(\frac{R_{cr}(0)T_c}{\sigma(T_c - T_{cl}^0)}\right)\right)}, \quad (11b)$$

where  $T_{cl}^0 \equiv T_{cl}(R = R_0)$  is the most probable transition temperature.

Using the distribution functions in the form of equations (8) or (11) one can average any physical property written as a function of the nanoparticle radius or temperature. For example, when calculating the dielectric permittivity, it is possible to average with  $f(R)$  and  $F(T_{cl})$  the expressions in the first and second lines, respectively, of equations (6). The results of the averaging are depicted in figures 2, 3. Figures 2 and 3 are built up respectively on the basis of the following equations:

$$\varepsilon(R_0, T) = \frac{\varepsilon_0(0)}{q |1 - t|} \int_0^\infty \frac{f(R) dR}{\sqrt{\left(1 - \frac{R_{cr}(T)}{R}\right)^2 + \delta^2}} \quad (12a)$$

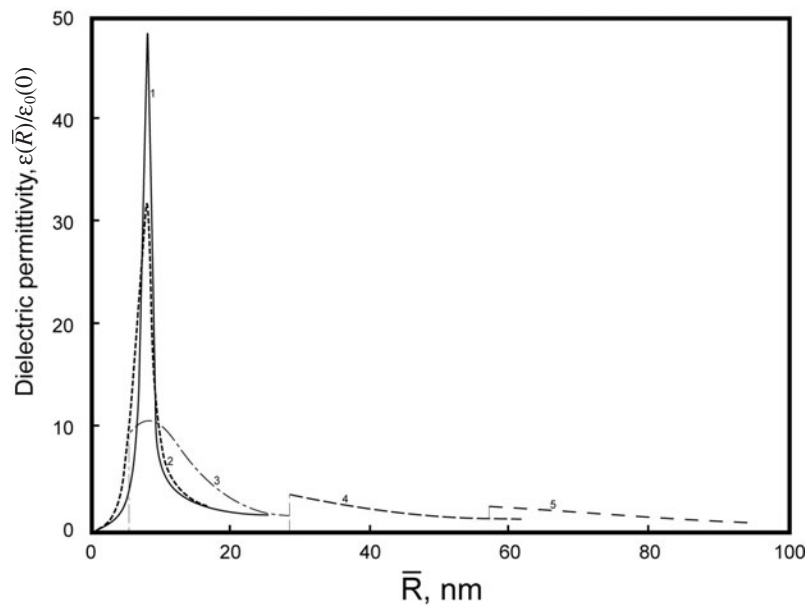


**Figure 2.** The dependence of the relative dielectric permittivity on the average grain size  $\bar{R}$  calculated on the basis of equations (12a), (8) for different dispersion parameters  $\sigma$ : 1 (1), 2 (2), 10 (3), 50 (4), 100 (5).

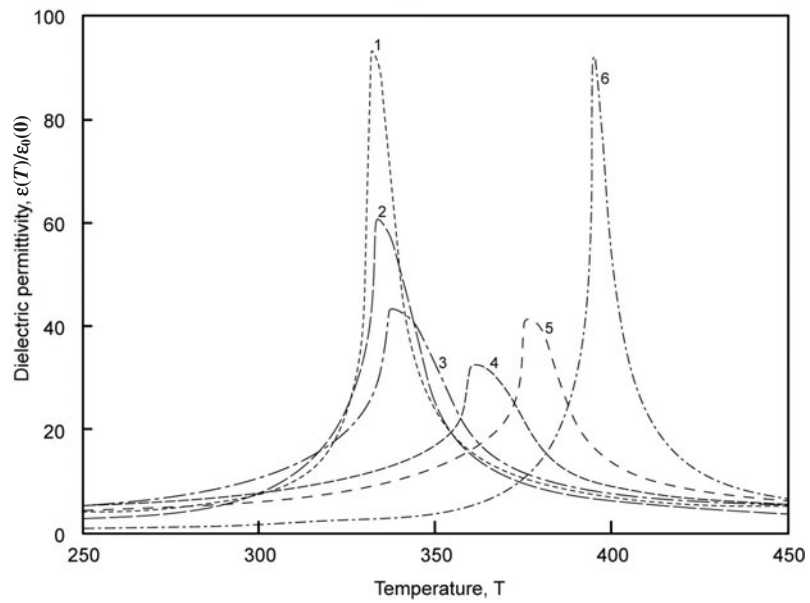


**Figure 3.** The dependence of the relative dielectric permittivity on the temperature, calculated on the basis of equations (12b), (11) for the following values of the parameter  $R_0/\sigma$ : 26 (1); 5.2 (2), 2.6 (3), 0.65 (4), 0.26 (5),  $5.2 \times 10^{-3}$  (6).

and

$$\varepsilon(t) = \frac{\varepsilon_0(0)}{q} \int_0^1 \frac{F(x) dx}{\sqrt{(t-x)^2 + \delta^2}}, \tag{12b}$$

**Table 1.** The experimental data and the parameters for the grain size distribution function extracted from the observed temperature dependence of the BaTiO<sub>3</sub> nanograin ceramic specific heat.

Experiment [10]	$\bar{R}$ (nm)	82.5	45.0	32.5	17.5
	$T_m$ (K)	393.0	385.8	372.0	332.5
	$\Delta T_{hw}$ (K)	0.3	5.2	7.8	8.1
Theory	$R_0$ (nm)	82.5	45.0	32.5	17.5
	$\sigma$ (nm)	4.000	7.168	5.302	1.807

where  $x \equiv \frac{T_{cl}}{T_c}$ ,  $t \equiv \frac{T}{T_c}$  and  $\delta = 0.01$  is a small parameter introduced to restrict the maximum height of the permittivity;  $q = 2$  and  $1$  for the ferroelectric and paraelectric phases, respectively;  $\varepsilon_0(0) = \frac{1}{\alpha T_c}$ . A more detailed discussion of the influence of the size distribution on the dielectric susceptibility and the peculiarities depicted in figures 2, 3 will be discussed later.

#### 4. Comparison of calculated and measured specific heat

To obtain a theoretical description of the temperature dependence of the specific heat observed for nanograin BaTiO<sub>3</sub> ceramics, we performed the averaging of equation (7) with the help of the distribution function  $F(T_{cl})$  in the form given by equations (11). That is, we carried out the calculation of the integral

$$\overline{\Delta C_p}(T_{cl}^0, T, \sigma) = \frac{\alpha^2 T}{2b} \int_0^{T_c} \frac{F(T_{cl}, T_{cl}^0, \sigma) dT_{cl}}{\sqrt{1 + \frac{4\alpha c}{b^2}(T_{cl} - T)}}. \quad (13a)$$

Using the relation between the half-width at half-height of  $f(R)$  and  $F(T_{cl}, T_{hw})$ , namely

$$\sigma \sqrt{\ln 2} = \frac{T_c \Delta T_{hw} R_{cr}(0)}{(T_c - T_{cl}^0)(T_c - T_{hw})}, \quad \Delta T_{hw} = T_{hw} - T_{cl}^0, \quad (13b)$$

it was possible to extract  $\sigma$  from the observed  $\Delta T_{hw}$  values and then  $R_0$  values from figure 1. The data and experimental parameters obtained are presented in table 1. They illustrate the possibility of extracting the parameters  $\sigma$  and  $R_0$  of the distribution function from experimental data. To obtain the  $\sigma$  and  $R_0$  values given in table 1 we took  $R_{cr}(0) = 4$  nm [10] and the values of  $T_{cl}^0$  were calculated on the basis of equation (3) at  $R = R_0$ .

In figure 4 we show the comparison of the calculated  $T_{cl}^0 = T_{cl \max} \equiv T_m$  with experimental data obtained for several  $\bar{R}$  sizes, for the case considered: small enough half-width that the value of  $R_0$  practically coincides with  $\bar{R}_{\max}$ . It can be seen from figure 4 that the theory fits the experimental points very well. It should be noted that although the measurements were performed on 500 nm BaTiO<sub>3</sub> films with different grain sizes, for films with thickness greater than 400 nm the specific heat practically coincides with that of the bulk (see [8, 9]), so 500 nm BaTiO<sub>3</sub> film can be considered as bulk ceramic.

Therefore, the only parameter that was taken from measurements of the specific heat is the value of the half-width  $\Delta T_{hw}$ , because  $T_{cl}$  can be calculated via  $R_0$ . In view of the first-order nature of the phase transitions in BaTiO<sub>3</sub>, we calculated the shift of the transition temperature as  $\Delta T_{cl}^0 = \frac{3}{16} \frac{b^2}{\alpha c} \approx 28$  °C for the values of parameters taken from [15] for BaTiO<sub>3</sub> bulk material. The results of the theoretical calculations on the basis of equations (13) using equations (11) and the values of  $\sigma$  given in table 1 are depicted in figure 5 as a solid curve. It can be seen that this line fits the experimental points fairly well. Note that the slope of the curves is related to the thermal capacity in the paraelectric phase ( $T > 400$  °C).

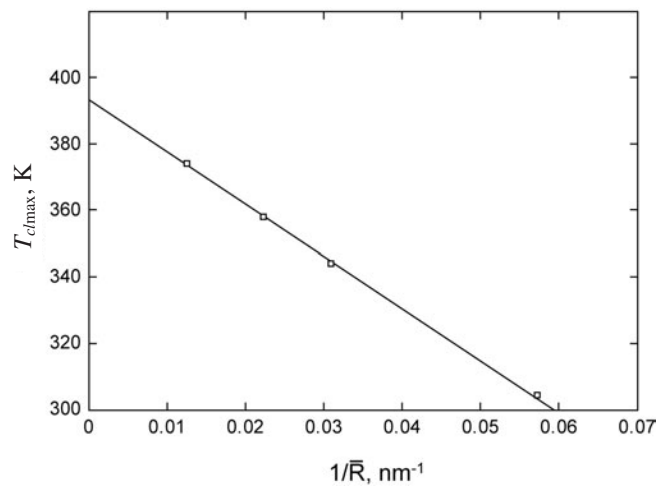


**Figure 4.** The dependence of the ferroelectric–paraelectric phase transition temperature on the inverse average grain size for BaTiO<sub>3</sub> nanograin ceramic. Solid line—theory; squares—experiment [10].

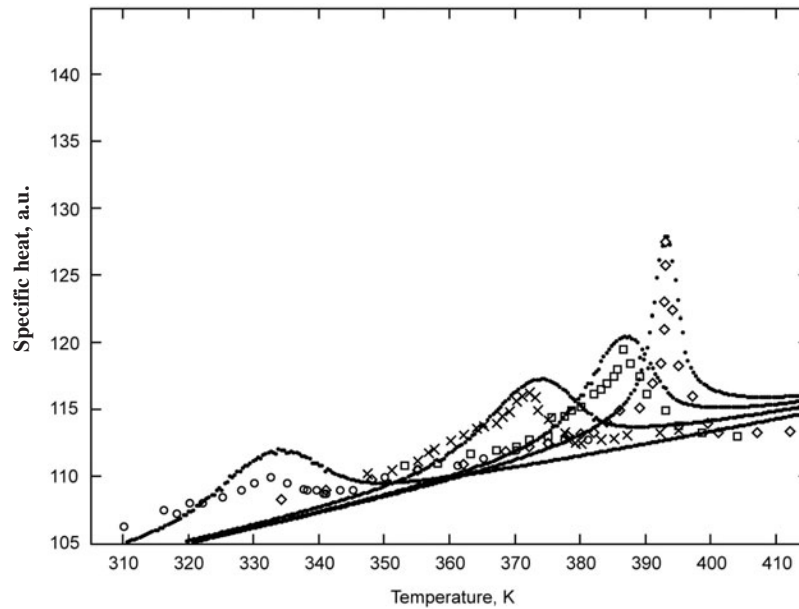


**Figure 5.** The temperature dependence of the specific heat for 500 nm BaTiO<sub>3</sub> films with different grain sizes, calculated on the basis of equations (11), (13) (solid curve) and experimental data taken from [10] for the following grain sizes: 35 nm (○), 65 nm (×), 90 nm (□), 165 nm (◇). The values of the experimental data and fitting parameters are given in table 1.

## 5. Discussion

### 5.1. Thin film roughness as a possible source of the transition parameter distribution

Experimental data obtained in [8, 9] for the temperature dependences of the BaTiO<sub>3</sub> specific heat for films with different thicknesses look like those for ceramics with nanosize grains



(see figure 5). In particular, it was shown that when the thickness of the film is reduced, the phase transition temperature decreases, while the smearing of the anomaly increases. The anomaly is quite weak for 40 nm film and it was not detected for 20 nm film. We draw attention to the fact that a sharp increase of the film roughness was revealed for the ultrathin films. In our view, the latter could be the reason for the diffusiveness of the specific heat anomaly near the thickness induced phase transition from the ferroelectric to the paraelectric phase in the thin films [8, 9]. Therefore, the distribution of the film thickness has to be taken into account when considering thin film properties. In particular, the calculations of the specific heat of the films can be performed similarly to the calculations in section 4 for nanograin ceramics, and allowing for the temperature of the thickness induced phase transition can be written in the following form [12]:

$$T_{cl} = T_c \left[ 1 - \frac{l_0^2(0)}{l} \left( \frac{1}{\lambda_1 + l_d} + \frac{1}{\lambda_2 + l_d} \right) \right]. \quad (14)$$

Here  $l_0^2(0) = \frac{\gamma}{\alpha_0 T_c}$ ,  $l_d^2 = \frac{\gamma}{4\pi}$  and  $l$ ,  $\lambda_1$ ,  $\lambda_2$ ,  $\gamma$  and  $\alpha_0$  are respectively the film thickness, the extrapolation length, the coefficient of the squared polarization gradient in the free energy functional and the inverse Curie–Weiss constant. Comparison of equations (14) and (3) shows that the dependences of  $T_{cl}$  on the particle size  $R$  and film thickness  $l$  are of the same type. Detailed calculations of the specific heat anomalies in thin films allowing for the difference in geometry of the films and nanoparticles are in progress now. The comparison of the calculated and observed anomalies will give valuable information about the parameters of the film thickness distribution function.

### 5.2. Influence of the size distribution function on the critical temperature and radius

It is generally believed that the critical temperature and radius of the size driven ferroelectric–paraelectric phase transition can be obtained from significant points for the properties, e.g. from the maximum of the dielectric permittivity. However, in real materials there is a distribution of transition temperatures  $T_{cl}$  (see equation (11a)) related to the distribution of sizes. In the general case the physical reason for the uncertainty as regards the physical meaning of the parameters which correspond to the observed property maxima is the competition between the distribution function and the positions of the property maxima. In particular, for the dielectric permittivity the maxima are at  $R = R_0$  and  $R = R_{cr}$  (see equations (8a) and (12a) respectively); so the distribution of the particle sizes makes it unclear whether the position of the observed  $\varepsilon(R)$  maximum has to coincide with the  $R_{cr}$  value. Let us consider this in more detail.

First of all, when the width of the distribution function is very small ( $\sigma \rightarrow 0$ ), i.e. it can be represented as a  $\delta$  function, there is only one  $T_{cl}$  value and so the positions of the  $\varepsilon(T)$  and  $\varepsilon(\bar{R})$  maxima do indeed define the critical temperature and critical radius respectively. This statement could hold for small enough  $\sigma \neq 0$  also. This situation, which is only found when using certain sample preparation techniques, did arise for the BaTiO<sub>3</sub> nanograin materials investigated in [8–10]. The latter is related to the quantitative criterion  $\bar{R} \approx R_0$  at  $R_0/\sigma \geq 1.5$  (see table 1). It follows from equation (9) that at  $\bar{R} \approx R_0$  the contribution of the second term can be neglected, similarly to the case for the limit  $\sigma \rightarrow 0$ . Therefore the criterion  $\frac{\bar{R}}{\sigma} \approx \frac{R_0}{\sigma} \geq 1.5$  can be considered as the condition for extracting critical parameters (temperature and radius) from the positions of the property maxima to be permitted; i.e. one can write the necessary relation between the distribution function parameters as

$$\sigma < \frac{2}{3} R_0. \quad (15a)$$

But for many real samples this criterion is not fulfilled. When  $\frac{R_0}{\sigma} < 1.5$  or  $\frac{\bar{R}}{\sigma} < 1.5$  the difference  $\bar{R} - R_0$  increases with increase of  $\sigma$ . Note that at  $R_0 \rightarrow 0$  average radius  $\bar{R} \rightarrow \frac{\sigma}{\sqrt{\pi}}$

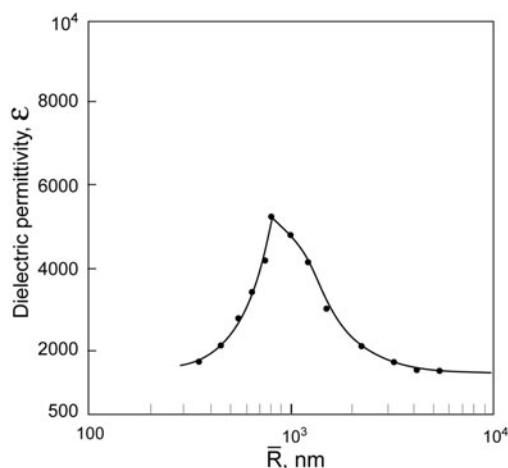


**Figure 6.** The size dependence of the dielectric permittivity for BaTiO<sub>3</sub> nanograin ceramics. Solid line—theory; points—experiment [11].

so that  $\bar{R}$  is restricted by this value; i.e.  $\bar{R}_{\min} = \frac{\sigma}{\sqrt{\pi}}$  (see figure 1). The same limit can be achieved at  $R_0 \neq 0$ ,  $\sigma \rightarrow \infty$ , giving  $\bar{R}_{\min} \rightarrow \infty$ . The latter case corresponds to bulk materials, while the former case shows that for nanomaterials there is a restriction on  $\bar{R}$  related to  $\sigma$  values. It is obvious that with increase of  $\sigma$ ,  $\bar{R}_{\min}$  can become larger than  $R_{\text{cr}}$ , so it can become impossible to extract  $R_{\text{cr}}$  from the experimental data. To obtain the actual value of  $R_{\text{cr}}$ , the size distribution function width has to satisfy the condition

$$\frac{\sigma}{\sqrt{\pi}} < R_{\text{cr}}(T). \quad (15b)$$

To illustrate this, we have depicted in figure 2 the dielectric permittivity ( $\varepsilon(\bar{R})$ ) dependence for  $R_{\text{cr}}(T = 196 \text{ K}) = 8 \text{ nm}$  [10]. It can be seen that condition (15b) is fulfilled for curves 1–3 and so their maxima positions correspond to  $\bar{R}_{\max} \approx R_{\text{cr}}(T)$ . Curves 4 and 5 are strongly shifted from the  $R_{\text{cr}}$  value, because for them  $\bar{R}_{\min} = \frac{\sigma}{\sqrt{\pi}}$  takes values of about 25 and 50 nm respectively, and these values are several times larger than  $R_{\text{cr}}(T) = 8 \text{ nm}$ .

It should be noted that conditions (15a) and (15b) coincide with one another at  $R_0 = \frac{3}{2}\sqrt{\pi}R_{\text{cr}}$ ; i.e.  $R_0$  must be about three times larger than  $R_{\text{cr}}$ . In addition, equation (15a) reflects the desirable qualities of nanograin ceramics, while equation (15b) is the necessary condition for it to be possible to extract the  $R_{\text{cr}}$  value from the observed size dependence of a property. In view of the fact that every  $\bar{R}$  corresponds to one sample with its own distribution function, defined by  $\sigma$  and  $R_0$  values, it is obvious that the curves depicted in figure 2 with fixed values of  $\sigma$  for every curve merely illustrate the size distribution role rather offering a description of any real experiment. On the other hand, we have shown by fitting the  $\varepsilon(\bar{R})$  dependence for BaTiO<sub>3</sub> nanoceramics observed in [11] with equations (12a), (8a) that condition (15a) is not satisfied for the majority of the  $\bar{R}$  points (although it is for two points in the ‘tails’ of the curve) and condition (15b) is not satisfied for any  $\bar{R}$  experimental values (see table 2 and figure 6), keeping in mind that for BaTiO<sub>3</sub>,  $R_{\text{cr}}(T = 300 \text{ K}) = 16 \text{ nm}$ . Note that when calculating the solid curve in figure 6 we used  $\delta = 0.001$  in equation (12a) and took the maximal intensity as a fitting parameter; this led to a fairly good description of all of the  $\varepsilon(\bar{R})$  values.

In the general case the condition (15b) is more restrictive than (15a). Therefore the essential dependence of the dielectric permittivity maximum position on the particles size distribution function width  $\sigma$  obtained and the estimation of conditions (15) can shed light upon the ‘puzzle’ of the much smaller (more than ten times smaller)  $R_{\text{cr}}$  value in nanopowder than in nanograin BaTiO<sub>3</sub> ceramics, derived from the observed  $\varepsilon(\bar{R})$  maxima position [11].

**Table 2.** The values of the parameters  $R_0$  and  $\sigma$  extracted from experimental data for  $\varepsilon(\bar{R})$  for BaTiO<sub>3</sub> nanograin ceramics with maxima around  $\bar{R} = 750$  nm [11].

$\bar{R}$ (nm)	350	450	550	650	750	1000	1250	1500	2250	3250	4250	5500
$\sigma$ (nm)	<100	150	350	550	850	1650	2000	1750	1750	2300	>2000	>2300
$R_0$ (nm)	350	450	541	599	562	159	324	1082	2126	3146	4250	5500

It should be stressed that conditions (15a) and (15b) are satisfied for the ceramics used for the specific heat measurements, as one can see from table 1.

In the temperature dependence  $\varepsilon(T)$ , a shift of  $T_{\max}$  to larger temperature with increase of  $\sigma$  was obtained again (see figure 3). While a decrease of the value of the maxima  $\varepsilon(\bar{R} = \bar{R}_{\max})$  with increase of  $\sigma$  was obtained for all of the  $\sigma$  values considered (see figure 2), the  $\varepsilon(T = T_{\max})$  values showed both decreases (see curves 1–4 in figure 3) and increases (see curves 5, 6 in figure 3) with increase of  $\sigma$ . The latter ‘peculiarities’ are related to the case  $T_{\text{cl}} \rightarrow T_c = 393$  K, as one can see from equation (11a), because larger  $\sigma$  values correspond to bulk material. Because of the distribution of  $T_{\text{cl}}$ , it only seems to be possible to extract from the experimental data the most probable transition temperature  $T_{\text{cl}}^0 = T_{\text{cl max}}$ . This was confirmed by specific heat measurements. Indeed, the  $T_m = T_{\text{cl max}}$  values obtained from the specific heat maxima positions (see table 1) were fitted fairly well by equation (3) at  $R = R_0 = \bar{R}_{\max}$  (see figure 4). From figure 3, for the temperature dependence of the dielectric permittivity one can see that the parameters  $R_0/\sigma$  for the curves 1–3 satisfy condition (15a), while the others do not satisfy it. One can also see that the  $T_m$  values for curves 1–3 are close to one another and to the value of  $T_{\text{cl}}^0$ , i.e. to the most probable transition temperature. This is similar to the specific heat case. In view of the fact that the different curves in figure 3 correspond to different samples with different values of  $\bar{R}$ , the smearing of curves 3, 4, which correspond to smaller  $\bar{R}$  values, looks like the behaviour of the specific heat also.

From the general point of view, the essential influences of the size distribution function characteristics  $\sigma$  and  $R_0$  on the dielectric susceptibility maximum position and height as well as on the specific heat open the way to the extraction of  $R_0$  and  $\sigma$  from experimental data, as was shown in section 4. These parameters are very important for the description of the properties of real nanomaterials and critical parameters of the size driven phase transition.

## References

- [1] Kosacki I and Anderson H U 2000 *Ionic* **6** 294
- [2] Kosacki I, Suzuki T, Petrovsky V and Anderson H U 2000 *Solid State Ion.* **136/137** 1225
- [3] Suzuki T, Kosacki I and Anderson H U 2002 *J. Am. Ceram. Soc.* **85** 1492
- [4] Ishikawa K, Yoshikawa K and Okada H 1988 *Phys. Rev. B* **37** 5852
- [5] Glinchuk M D and Morozovskaya A N 2003 *Phys. Status Solidi* **238** 81
- [6] Shih W Y, Shih W H and Askay I A 1994 *Phys. Rev. B* **50** 15575
- [7] Bottcher R, Klimm C, Michel D, Semmelhack H C, Volkel G, Glasel H I and Hartmann E 2000 *Phys. Rev. B* **62** 2085
- [8] Davitadze S T, Kravchun S N, Strukov B A, Goltzman B M, Lemanov V V and Shulman S G 2002 *Appl. Phys. Lett.* **80** 1631
- [9] Strukov B A, Davitadze S T, Kravchun S N, Taraskin S A, Goltzman N, Lemanov V V and Shulman S G 2003 *J. Phys.: Condens. Matter* **15** 4331
- [10] Strukov B, Davitadze S T, Shulman S G, Goltzman B M and Lemanov V V 2004 *Preprint cond-mat/0405224*
- [11] Niepce J C 1994 *Electroceramics* **4** 29
- [12] Glinchuk M D, Eliseev E A and Stephanovich V A 2002 *Physica B* **322** 356
- [13] Glinchuk M D, Eliseev E A, Stephanovich V A and Farhi R 2003 *J. Appl. Phys.* **93** 1150
- [14] Hudson D J 1964 *Statistics for Physicists* (Geneva) (1967 (Moscow: Mir))
- [15] Lines M E and Glass A M 1977 *Principles and Applications of Ferroelectrics and Related Materials* (Oxford: Clarendon)